International Journal of Engineering and Advanced Technology (IJEAT)
ISSN: 2249-8958 (Online), Volume-6 Issue-6, August 2017

Low Resolution to High Resolution Image Projection with Spectral, Noise Removal and Edge Preservation Coding Techniques

M. Nagaraju Naik, P. Raveendrababu

***Abstract:** Many technical papers were presented in the improvement of accuracy and visual quality. Image coding is developed over a long period with various enhancement techniques. In the area of digital image processing resources required in optimized methods for better representation of higher resolutions for progressive image processing. More research work required towards high-resolution representation in real time applications and focused more optimization methods for efficient system representation. But available resources are limited due to noise, due to the noisy overall system accuracy and efficiency will decrease. Fourier transform represents less accuracy and visual quality because projecting energy with noise in all the directions. Hence we propose a lower dimensional coding system with higher accuracy with spectral band interpolation; inter-frame correlative for noise removal and finally adaptive edge preservation for smooth representation. The proposed technique gives more accuracy and projected in the higher grid and hence the obtained system is robust.*

***Keywords:** Accuracy, Interpolation, Image Coding, Spectral Band, Edge Preserving*

I. INTRODUCTION

High resolution representations are required for real time applications, like HDTV, Video conference, live streams and image representation. The projection is required to project a higher grid for better representation. An interpolation technique is the one of the technique to project in a higher grid. To achieve higher visual quality the stated interpolation approaches were carried out in the frequency representation using interpolation techniques [1], [2]. The predominantly used interpolation is the Fast Fourier-based interpolation [3] technique. It is observed that Fourier transformation transforms the image data from the time domain to frequency domain with non-resolution description resulting in lower accuracy in image interpolation. During the interpolation of image sequence from low resolution to high resolution the projection is carried out in 2D projection, which resulted in poor visual quality, because noise also projected. For projecting an image in 2-D, a cubic B-spline method [4] proposed for low resolution image.

Manuscript published on 30 August 2017.
* Correspondence Author (s)
Dr. M. Nagaraju Naik, Associate Professor, Department of Electronics & Communication Engineering, CMR College of Engineering & Technology, Kandlakoya (Hyderabad), India. E-mail: nagarajunaik1976@cmrcet.org
P. Raveendrababu, Associate Professor, Department of Electronics & Communication Engineering, CMR College of Engineering & Technology, Kandlakoya (Hyderabad), India. E-mail: praveendrababu@cmrcet.org

The adaptive Wiener filter (AWF) [5], [6] was initially developed for grayscale imaging and has not been applied to color SR coding. In this approach, a novel fast SR method for CFA cameras based on the AWF SR algorithm is used as global channel-to-channel statistical models. This new method defined as a stand-alone algorithm, also taken as an initialization approach for a variational SR algorithm. To preserve edges proposed bilateral filtering approach [7]. Preservation of edges is important for an interpolated video (smoothness) otherwise it degrades the visual quality. This approach presents a new sharpening and smoothing algorithm [8] based on the application of adaptive bilateral filter (ABF) on the edges extracted. A multi-resolution analysis is used to approximate the edges with lower coefficients compared to wavelet transform and this method suffers from unwanted frequency components due to interpolation. The image and video reconstruction algorithm using spline interpolation was proposed in [9], [10] using the single frame. Early works on interpolation consider the transformation of non-uniform samples in uniform samples using the concept of the sampling theorem [11] without loss of data by satisfying the Nyquist theorem.

The HR image or video was reconstructed using a single low resolution, frame with pair matching. This algorithm requires a large collection of database and storage space. [12] Proposed an algorithm for video super resolution using the quality coefficients for an accurate motion estimation and a number of LR frames required by this algorithm is 8 to 16. In this algorithm FFT based image registration technique is used and this method is sensitive to noise and it works for only global rotation. Based on kernel regression and spatial-temporal orientation a super resolution algorithm is proposed in [13] According to this method kernel regression is the best way to use irregular interpolation and this method causes loss of edges and border information. Super resolution reconstruction is an inverse problem which is effectively eliminated by regularization of an image is proposed in [14] with bilateral total variance. This algorithm suffers due to smooth output and loss of edges. According to this algorithm, a high-order prediction is used to find the sub-pixel motion with structural similarity features. In [15], [16], proposed a self-adaptive blind super-resolution image reconstruction approach which is based on multiple images and proposed method can adaptively choose the parameter of regularization term [17], [18, 19]. The quality of the resulting image, especially in respect of edge-preserving property is better than approaches such as maximum a posteriori estimation (MAP) tested with practical examples [20].

II. PAST WORK

The earlier approaches considered a still-image scenario, although many do not necessarily limit to video. High resolution (HR). is the process of combining a sequence of low resolution images in order to produce a higher resolution image. The objective of super resolution, as its name suggests, is to increase the resolution of an image. Resolution is a measure of frequency content in an image, high resolution (HR) images are band limited to a larger frequency range than low-resolution (LR) images. There are many algorithms and methods developed to produce a super resolution imaging [1], [2]. In [3], [4] provides a basic approach of super resolution, different methods for image reconstruction based on frequency and spatial domain. There is a great demand for the quality of medical images or video sequences for accurate processing of various fields of applications, Magnetic Resonance Imaging (MRI) can only acquire images and video sequence with low resolution [5]. In [6], [7], [8] a special case of the high resolution problem was concentrated, where the coding is composed of pure translation and rotation, the blur is space invariant and the noise is additive white Gaussian noise. In [9] [10], [11] a weighted median filtering for refinement process is supported, it is observed that with this refinement, even the simple box filter aggregation achieves comparable accuracy with various sophisticated aggregation methods (with the same refinement). The adaptive Wiener filter (AWF) [12], [13] was initially developed for gray scale imaging and has not been applied to color SR coding. In [14], [15] presents an edge-enhancing super-resolution algorithm using anisotropic diffusion technique. In addition to reducing image noise during the restoration process, this method helps to enhance the edges. a novel algorithm for single image super resolution is proposed. Back-projection can minimize the reconstruction error with an efficient iterative procedure. Promising results can be obtained by the proposed bilateral back-projection method efficiently. In [16], the adaptive bilateral filter (ABF) for to enhance CT images by applying half-quadratic edge-preserving image restoration (or de-convolution) to them is proposed. The method focuses on numerical efficiency and developed a fast implementation based on a simple three dimensional MRF model with convex edge-preserving potentials in [17], [18] [19]. The resulting restoration method yields good recovery of sharp discontinuities while using convex duality principles yields fairly simple implementation of the optimization. In [20], [21] a novel directionally adaptive image resolution enhancement method was proposed. enhancement of sharpness and noise removal is presented.

III. PROJECTION

The pixel to be projected is needed to be placed at the correct grid points so as the projection is done accurately, however, in present methods [1] projection is done based on a pixel by pixel mapping, such method introduces redundancy (repetition of the pixel values) it results in poor visual quality. To improve the projection accuracy, rather project pixel by pixel performing frequency domain using FFT, over the FFT of the image, the pixel energies are obtained. These pixel energies are used for projection. However, coming to real time application the energy variation is not equal in all directions, horizontal, vertical, diagonal and approximation. Sometime *x* variation will be higher than *y* and *z*, and vice versa, hence it cannot be asserted said that all direction variables will be equal, and hence visual quality is decreased. Therefore the FFT approach needs improvement.

IV. INTERFRAME CORRELATION

In image and video noises are added up, due to the processing system, medium or algorithms, which are very practical in real time, whereas these noises are also projected. Noise projection degrades the visual quality. Hence, only projection algorithm accuracy is not sufficient to achieve higher accuracy. The accuracy of input data is also required prior to projection it is pertinent to remove any noise that is present. To denoise, the LR sample Wiener based coding is presented. However, this approach has two limitations,

i) The method is non-adaptive with respect to noise effect; hence noises with time varying nature can't be effectively removed.

ii) When projecting in planar mode, i.e. in 3 directions, (H, V, D), such filteration approach as is not defined.

Hence an inter frame correlation technique is proposed to overcome the Wiener filter disadvantages.

V. EDGE PRESERVING

The earlier two proposed approaches enabled us to achieve better projection besides a noise-free projection. However, during the process of projection and filteration, sharp variations at the edges are lost, which resulted in degradation of visual quality. Therefore, focus is on new methodologies for filteration with adaptive edge preserving as our third objective. To preserve edge information among various methods bilateral filteration approach was defined in [21] is more prominently being used, due to its lower computational complexity? However, this method is defined only for single images for the filteration process. No such work was stated to have been observed towards the application of bilateral filteration in interpolation approach. While applying bilateral filteration for interpolation, the basic problem observed is the dynamic variation of each energy projection. As the projecting coefficients are predicted which was obtained from mathematical computations and as no prior filteration coefficient could be defined.

VI. PROPOSED SYSTEM

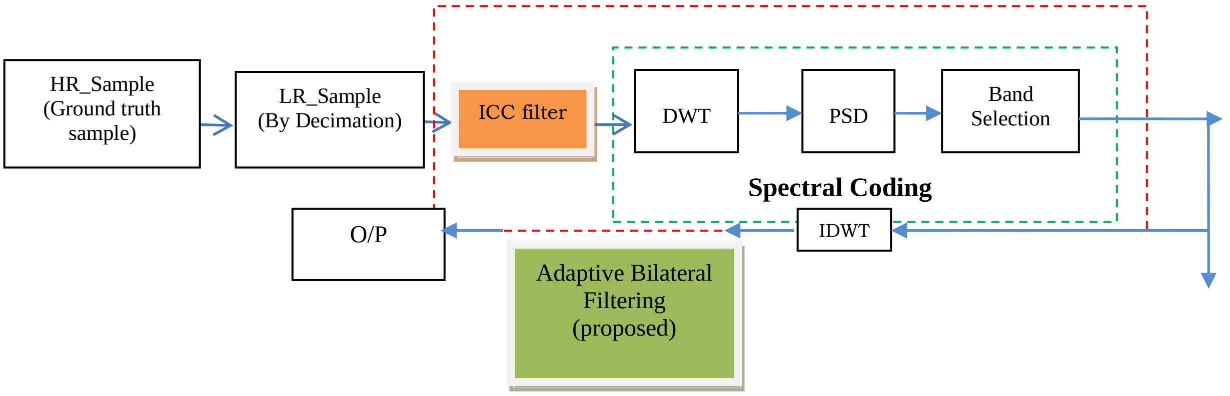

Figure 1: Proposed hybrid architecture system

First considered HR sample also called ground truth sample and converting into LR sample using downsampling for easy processing, and reducing the dimensionality and then applying the DWT technique and interpolating the image and finally applying the IDWT for getting the original image. But in the proposed method of application, the spectral coding method and interpolation are used or better reconstruction of original images. In this proposed approach, each image is decomposed into 3 fundamental resolutions (x,y,z) (i.e. H,V,D) for each resolution absolute energy is computed by using PSD (power spectral density) and these PSD values are used for projections. Later an IDWT is applied to get back the projected pixel in a time domain. This approach, processed in individual planes, they are more accurate and result in better visual quality. In the process of DWT based interpolation, a 2D-DWT is computed by performing low-pass and high pass filteration of the image coefficients take place as shown in Figure 2. A low-pass and high-pass filter are defined and denoted by *h(n)* and *g(n)*, to perform a pyramidal decomposition of the image coefficient. At each level, the high-pass filter generates detailed information from the processing sample, while the low-pass filter produces the coarse approximations of the input image. At the end of each low-pass and high-pass filteration, the outputs are down-sampled by two (↓2) to obtain a dimensional reduction of the processed coefficients. In order to compute a 2D-DWT, the decomposition is performed twice in both horizontal and vertical directions. In a 2D-DWT operation, a 1D-DWT is carried out over, each row, which is referred to as horizontal filtering of the image followed by a 1D-DWT on each column, which is called vertical filtering.

The PSD for a given signal x(t) is defined as,

$$PSD, P = \lim_{T\to\infty} \frac{1}{2T} \int_{-T}^{T} x(t)^2 \, dt \qquad (1)$$

bands are selected based on a defined selection criterion, as outlined. For the obtained PB_i, maximum PB is computed, defined by,

$MPB_i = \max(PB_i)$

For $i = 1$ *to* 4

if $(PB_i \geq (MPB_i / 2))$

$sel\_B_i = B_i$;

end

These selected bands, 'Sel_B_i' are then used for interpolation in the high resolution grid. The coefficients are mapped to required scale grid and inverse transformation is carried out to recover the video frame back. Though this interpolation approach has an advantage of higher resolution coding the noise interpolation is to be minimized. To meet the process objective of noise minimization, a filteration logic following inter frame correlation logic is presented.

The estimated error is then defined as;

$$e_{i,H}(k) = H_{i,t}(k) - H_i(k)w(k) \qquad (2)$$

the error has recursively been computed over the total frames (i=1….N), and the initial error is recorded as $e_{i,H,init}$.

A weight factor is then updated as,

$$w(k+1) = w(k) + \mu \sum_{i=0}^{N-1} \frac{H_i^T(k)}{\|H_i(k)\|^2} e_{i,H,init}(k) \qquad (3)$$

where μ is the updating step size, with an error updating factor. Various methods were proposed in the literature to regularize the inverse problem. Two of the most extensively explored image modelling approach is the image smoothness approach and the edge smoothness approach. Simple filtering or interpolation algorithms (*e.g.*, bilinear/bi-cubic interpolation) can produce smooth, high resolution images, which are usually blurry, thus have limited image quality. To preserve edge sharpness, edge directed interpolation is proposed to prevent cross-edge interpolation. The ringing artifacts are found more dominant. To achieve the objective of efficient image projection preserving image edge in this chapter a feedback model for edge preserved coding based on Adaptive–Bilateral Filteration (ABF) is suggested.

Published By:
Blue Eyes Intelligence Engineering
and Sciences Publication (BEIESP)

In this section, we present an acute and smoothing algorithm: the adaptive bilateral filter (ABF). The response at $[m_0, n_0]$ of the proposed shift-variant ABF to an impulse at [m,n] is given by equation (5.5)

$$h[m_0,n_0;m,n] = \begin{cases} r_{m_0,n_0}^{-1} \exp\left(-\frac{(m-m_0)^2+(n-n_0)^2}{2\sigma_d^2}\right) \exp\left(-\frac{(g[m,n]-g[m_0,n_0]-\varsigma[m_0,n_0])^2}{2\sigma_r^2}\right), [m,n] \in \Omega_{m_0,n_0} \\ 0, \quad else \end{cases} \quad (4)$$

and normalization factor is given as

$$r_{m_0,n_0} = \sum_{m=m_0-N}^{m_0+N} \sum_{n=n_0-N}^{n_0+N} \exp\left(-\frac{(m-m_0)^2+(n-n_0)^2}{2\sigma_d^2}\right) \times \exp\left(-\frac{(g[m,n]-g[m_0,n_0]-\varsigma[m_0,n_0])^2}{2\sigma_r^2[m_0,n_0]}\right), \quad (5)$$

The ABF retains the general form of a bilateral filter, but contains two important modifications. First, an offset ζ is introduced to the range filter in the ABF. Second, both ζ and the width of the range filter σ_r in the ABF are locally adaptive. If ζ=0 and σ_r is fixed, the ABF will degenerate into a conventional bilateral filter. For the domain filter, a fixed low-pass Gaussian filter with σ_d is adopted in the ABF. The combination of a locally adaptive ζ and σ_r transforms the bilateral filter into a much more powerful filter that is capable of both smoothing and sharpening.

We will demonstrate the effect of bilateral filtering with a fixed domain Gaussian filter ($\sigma_{d=1.0}$) and a range filter ($\sigma_{r=20}$) shifted by the following choices for ζ

1) No offset (conventional bilateral filter): $\zeta[m_0, n_0] = 0$.
2) Shifting towards the MEAN : $\zeta[m_0, n_0] = -\Delta_{m_0,n_0}$
3) Shifting away from the MEAN: $\zeta[m_0, n_0] = \Delta_{m_0,n_0}$
4) Shifting away from the MEAN, to the MIN/MAX

$$\zeta[m_0, n_0] = \begin{cases} MAX(\Omega_{m_0,n_0}) - g[m_0,n_0], if\, \Delta_{m_0,n_0} > 0 \\ MIN(\Omega_{m_0,n_0}) - g[m_0,n_0], if\, \Delta_{m_0,n_0} < 0 \\ 0 \quad , if\, \Delta_{m_0,n_0} = 0 \end{cases} \quad (6)$$

The parameter of the range filter controls the width of the range filter. It determines how selective the range filter is, in choosing the pixels that are quite similar in gray value to be included in the averaging operation. If σ_r is large compared to the range of the data in the window, the range filter will assign similar weight to every pixel in the range. Consequently, it will not have much effect on the overall bilateral filter. On the other hand, a small σ_r will make the range filter over takes the bilateral filter. The bilateral filtered image resembles the range filtered image, and it resembles the domain filtered image when $\sigma_{r=5}$ and it resembles the domain filtered image when $\sigma_{r=50}$.

A. Performance Parameters

1. Mean squared error (MSE)

$$MSE = \frac{1}{MXN} \sum (f - \hat{f})^2 \quad (7)$$

2. Peak signal-to-noise ratio (PSNR)

$$PSNR(dB) = 10log_{10}\left(\frac{I_{peak}^2}{MSE}\right) \quad (8)$$

3. Structural Similarity Index Measurement (SSIM)

$$SSIM = \frac{\sum_i \sum_i f(i,j) \otimes f_w(i,j)}{\sum_i \sum_i (f(i,j))^2} \quad (9)$$

4. Route Mean square Error (RMSE)

$$RMSE = \sqrt{MSE} \quad (10)$$

5. Relative Reconstruction Error (RRE)

$$RRE = \frac{\sqrt{\sum\sum r(x,y) - t(x,y)^2}}{\sum\sum r(x,y)^2} \quad (11)$$

VII. EXPERIMENTAL RESULTS AND DISCUSSIONS

Considered four different image samples for testing and verification of performance they are the Tower, Lena, Boat and Tajmahal.

a) b) c) d)

Figure 2: Test image samples a) Tower (S1), b) Lena (S2), c) Boat (S3), d) Tajmahal (S4)

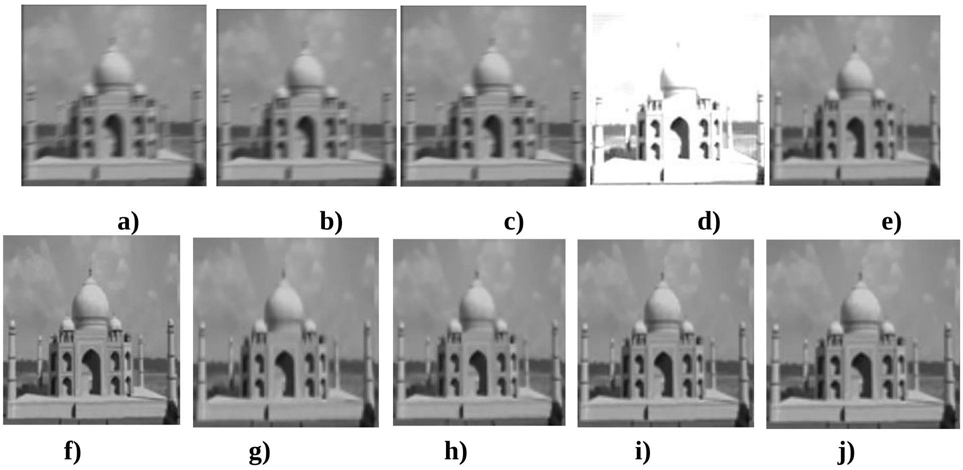

Figure 3 : Interpoltaed frame of Tajmahal (a) NNG, (b) BL, c) BC, d) FFT, e) Spline, f) SC, g) W-SC, h) ICC-SC, i) BF, j) ABF

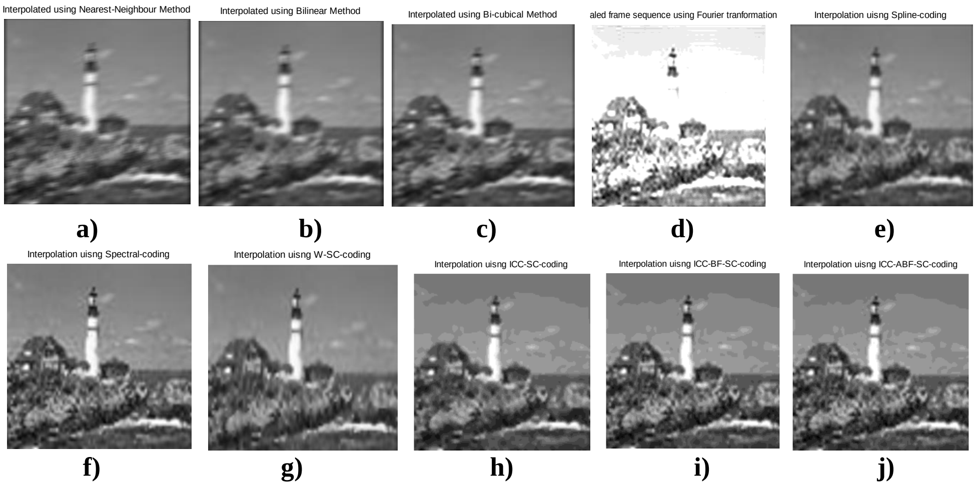

Figure 4: Interpolated tower image using a) NNG, b) BL, c) BC, d) FFT, e) Spline, f) SC, g) W-SC, h) ICC-SC, i) BF, j) ABF

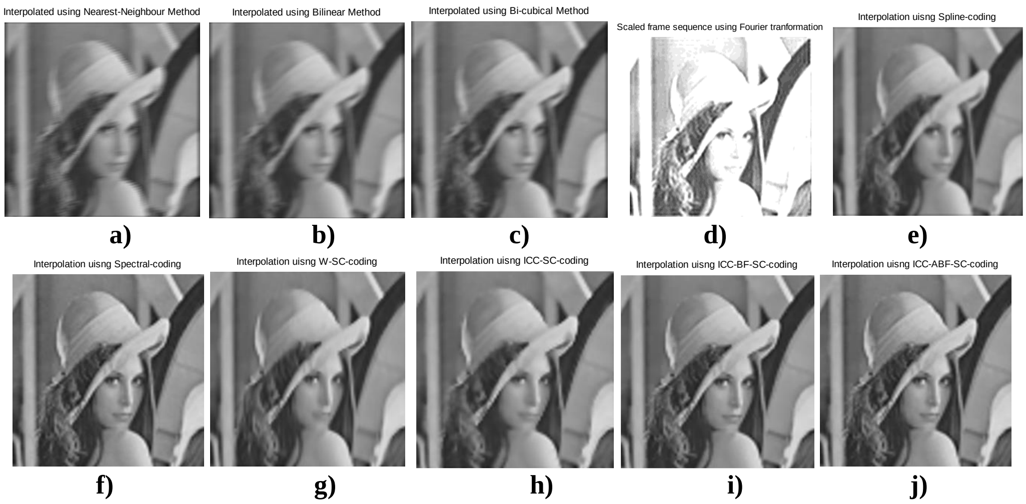

Figure 5 : Interpolated Lena image samples using a) NNG, b) BL, c) BC, d) FFT, e) Spline, f) SC, g) W-SC, h) ICC-SC, i) BF, j) ABF

Published By:
Blue Eyes Intelligence Engineering and Sciences Publication (BEIESP)

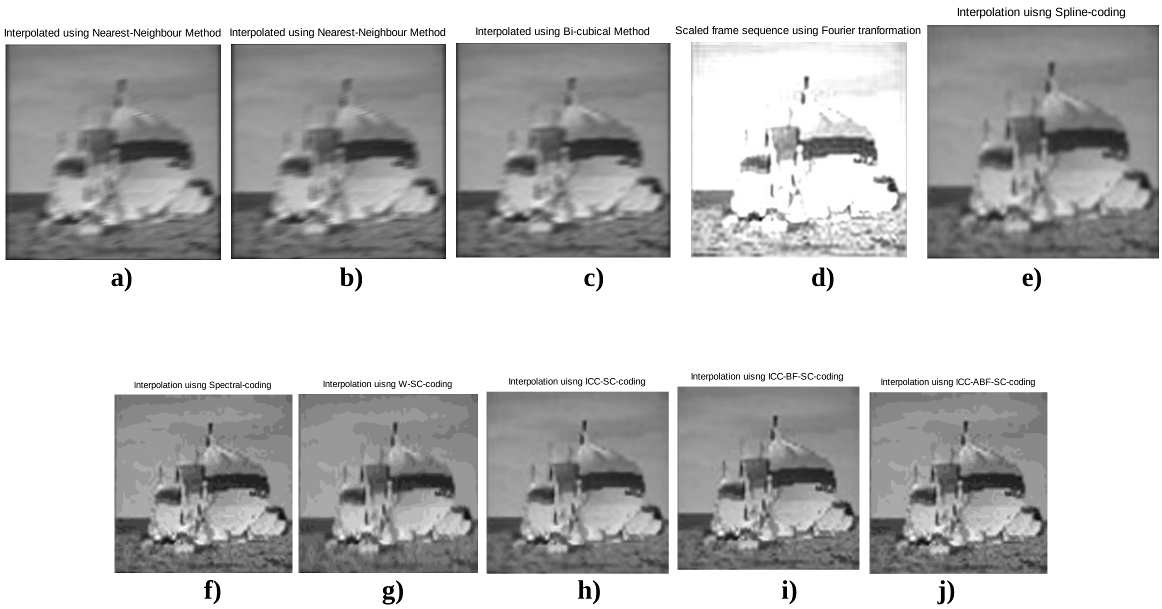

Figure 6: Interpolated Lena image samples using a) NNG, b) BL, c) BC, d) FFT, e) Spline, f) SC, g) W-SC, h) ICC-SC, i) BF, j) ABF

Performance Tables and Graphs:

Table 1: Performance evaluation of PSNR

Methods	PSNR			
	S1	S2	S3	S4
NNG	28.25	30.25	28.25	29.60
BL	29.25	31.25	29.25	30.03
BC	30.56	33.56	29.56	30.49
Fourier	30.25	34.25	30.25	30.68
Spline	31.45	35.45	30.45	31.65
SC (Proposed)	**31.55**	**35.55**	**30.55**	**32.21**
W-SC	32.20	36.80	31.52	35.63
ICC-SC (Proposed)	**35.12**	**37.56**	**33.85**	**37.42**
BF	36.16	40.25	34.15	38.15
ABF(Proposed)	**38.15**	**43.56**	**36.52**	**39.42**

The above table represents the evaluation of PSNR and it is observed that the Lena sample got more peak signal to noise ratio i.e. 13.31 compare to nearest neighbor.

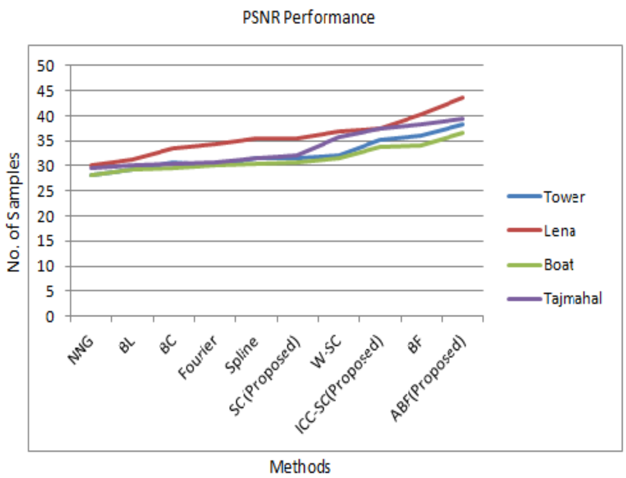

Figure 7: Performance graph of PSNR

The above graph represents the performance of PSNR and it is observed that Lena sample got the higher peak signal to noise ration compare to other samples.

Table 2: Performance evaluation of MSE

Methods	MSE			
	S1	S2	S3	S4
NNG	39.55	46.55	41.55	85.26
BL	38.55	45.55	40.55	81.84
BC	37.25	44.25	39.25	75.34
Fourier	36.25	43.25	39.25	71.39
Spline	35.26	42.26	38.26	65.25
SC (Proposed)	**34.26**	**42.26**	**37.26**	**55.33**
W-SC	33.26	41.52	36.41	40.91
ICC-SC (Proposed)	**25.13**	**27.13**	**30.12**	**32.76**
BF	20.15	19.23	36.12	25.10
ABF(Proposed)	**16.23**	**10.26**	**19.56**	**19.03**

The above table represents the evaluation of Mean square error and it is observed that the Lena sample obtain a less mean squared error (MSE) i.e. 36.29 compare to nearest neighbor.

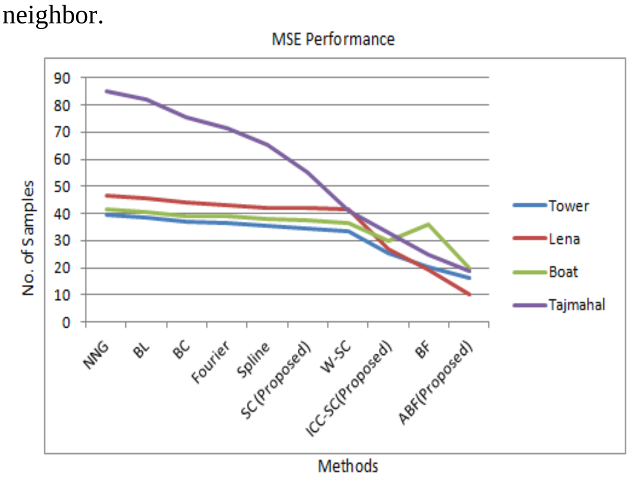

Figure 8: Performance graph of MSE

Published By:
Blue Eyes Intelligence Engineering and Sciences Publication (BEIESP)

The above graph represents the performance of MSE and it is observed that Lena sample obtained less mean squared error compare to other samples.

Table 3: Performance evaluation of RMSE

Methods	**RMSE**			
	S1	S2	S3	S4
NNG	11.74	12.74	12.74	9.23
BL	10.74	11.74	11.74	9.04
BC	9.03	10.03	10.03	8.67
Fourier	8.64	9.64	9.64	8.44
Spline	7.87	8.87	8.87	8.07
SC (Proposed)	**6.69**	**7.69**	**7.69**	**7.43**
W-SC	5.76	6.44	6.03	6.39
ICC-SC(Proposed)	**5.01**	**5.20**	**5.48**	**5.72**
BF	4.48	4.38	5.11	5.01
ABF(Proposed)	**4.02**	**3.20**	**4.42**	**4.36**

The above table represents the evaluation of RMSE and it is observed that the Lena sample got less RMSE i.e. 9.54 compare to nearest neighbor.

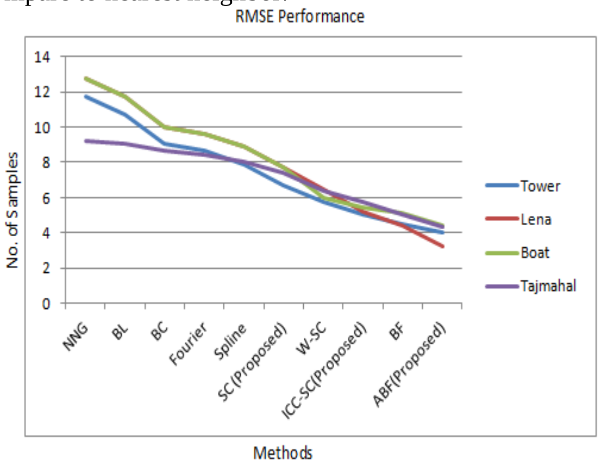

Figure 9: Performance graph of RMSE

The above graph represents the performance of RMSE and it is observed that Lena sample obtained less RMSE compare to other samples.

Table 4: Performance evaluation of RRE

Methods	RRE			
	S1	S2	S3	S4
NNG	0.112	0.098	0.085	0.1064
BL	0.102	0.092	0.082	0.1037
BC	0.101	0.091	0.081	0.0952
Fourier	0.096	0.086	0.076	0.0786
Spline	0.091	0.081	0.071	0.0658
SC (Proposed)	**0.088**	**0.078**	**0.068**	**0.0523**
W-SC	0.078	0.065	0.067	0.0452
ICC-SC(Proposed)	**0.066**	**0.057**	**0.036**	**0.0439**
BF	0.060	0.031	0.032	0.036
ABF(Proposed)	**0.055**	**0.021**	**0.025**	**0.030**

The above table represents the evaluation of relative reconstruction error and it is observed that the Lena and boat sample got less RRE i.e. 0.077 compare to nearest neighbor.

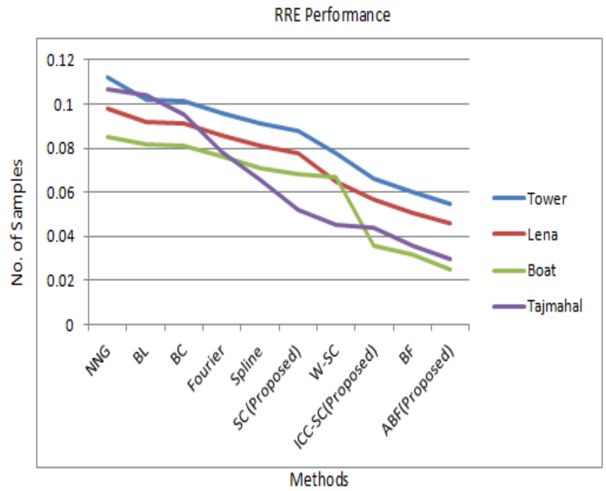

Figure 10: Performance graph of RRE

The above graph represents the performance of RRE and it is observed that the Lena and boat samples got less RRE compare to other samples.

Table 5: Performance evaluation of SSIM

Methods	SSIM			
	S1	S2	S3	S4
NNG	0.525	0.625	0.525	0.453
BL	0.425	0.525	0.425	0.484
BC	0.475	0.575	0.475	0.525
Fourier	0.515	0.615	0.515	0.562
Spline	0.565	0.665	0.565	0.594
SC (Proposed)	**0.577**	**0.677**	**0.577**	**0.655**
W-SC	0.678	0.746	0.665	0.693
ICC-SC(Proposed)	**0.725**	**0.793**	**0.702**	**0.715**
BF	0.775	0.846	0.746	0.765
ABF(Proposed)	**0.841**	**0.894**	**0.792**	**0.805**

The above table represents the evaluation of the structural similarity index and it is observed that the Lena sample got higher structural similarity i.e. 0.269 compare to nearest neighbor.

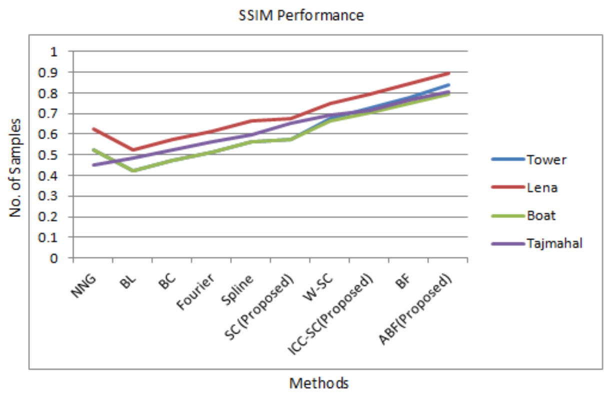

Figure 11: Performance graph of SSIM

The above graph represents the performance of the structural similarity index, and it is observed that Lena sample got higher structural similarity compare to other samples.

Published By:
Blue Eyes Intelligence Engineering
and Sciences Publication (BEIESP)

VIII. CONCLUSION

The spectral resolution projection is carried out in low dimensional and the image is projected to a higher grid based on energy distribution. A Spectral Coding (SC) method is proposed to improve resolution accuracy. It is observed that the proposed approach is evaluated in various test samples and ascertained similar improvement. An inter correlative coding technique for removal of noise and improvement of resolution accuracy. They are found to be relatively improved when compared to the spectral coding technique. The quality of restored image is significantly improved when compared to conventional bilateral filteration. By using Adaptive filteration the ringing artifacts noticed at the edges were eliminated while interpolating the receiving side. This approach enables improvement of the processing efficiency for image projection. It is also observed that for Lena sample obtained highest performance value compared to other techniques.The PSNR increased 6dB, the the decrement of MSE with 36.29, decrement of RMSE with 9.54, the decrement of RRE with 0.077, the increment of SSIM with 0.269. Hence proposed system achieved better results compared to other approaches and it is robust for image projections. out of three image samples Lena sample has secured best PSNR, MSE besides other factors.

REFERENCES

1. P. Vandewalle, S. Su and M. Vetterli etal, “A frequency domain approach to registration of aliased images with application to super-resolution”, EURASIP Journal on Advances in Signal Processing, vol.6, 2006.
2. S. C. Park, M. K. Park, and M. G. Kang, “Super-resolution image reconstruction: a technical overview”, Signal Processing Magazine, IEEE, vol. 20(3), pp. 21–36, 2003.
3. Deepesh Jain, “Super resolution using Papoulis-Gerchberg Algorithm”.
4. N. Bharati, A. Khosla and N. Sood, “Image reconstruction using cubic b-spline interpolation”, India Conference(INDICON), Annual IEEE, pp. 1–5, 2011.
5. Kwok-Wai Hung,Wan-Chi Siu, “Single Image Super Resolution using Iterative Wiener Filter”, ICASSP, IEEE, 2012.
6. T. Tajbakhsh, “Combined Demosaicing and Adaptive Filtering on CFA Images”, IEEE Tenth International Symposium on Consumer Electronics, ISCE '06, 2006.
7. J. Allebach and P. W. Wong, “Edge-Directed Interpolation”, in ICIP, 1996.
8. YunfeiBai, Jing Hu, YupinLuo, “Self-Adaptive Blind Super-Resolution Image Reconstruction”, 3rd International Congress on Image and Signal Processing (CISP2010), 2010.
9. S. KumarMaurya, P. KumarMishra, R. KumarSingh and A. Kumar Misra, “Image enhancement by spline interpolation and adaptive power spectrum cut-off of filtered images”, in Advances in Engineering, Science and Management(ICAESM), International Conference on. IEEE, pp.423–428, 2012.
10. H. A. Aly and E. Dubois, “Specification of the observation model for regularized video up-sampling,” IEEE Trans. Video Processing, vol. 14, pp. 567-576, May 2005.
11. Y.-M. Zhu, “Generalized sampling theorem”, Circuits and Systems II: Analog and Digital Signal Processing, IEEE Transactions, vol. 39(8), pp. 587–588, 1992.
12. M.Irani and S.Peleg, “Motion analysis for image enhancement: resolution, occlusion and transparency”, JVCIP, 1993.
13. S. Izadpanahi, “Motion based video super resolution using edge directed interpolation and complex wavelet transform”, signal processing, Elsevier, vol. 93(7), pp. 2076-2086, 2013.
14. Wong, “Adaptive Bilateral Filtering of Image Signals using Local Phase Characteristics”, Signal Process. (Elsevier), Vol. 88, pp.1615, 2008.
15. Xiuju Liang, ZongliangGan, “Improved Non-Local Iterative Back Projection Method for Image Super-Resolution”, Sixth International Conference on Image and Graphics, ICIG, 2011.
16. J. Storkey, “Dynamic structure super-resolution”, Advances in Neural Information Processing Systems, pp.1319–1326, 2003.
17. T. Mitsunaga and S.K. Nayar, “Radiometric self-calibration”, in Proc. IEEE Int. Conf. Computer Vision and Pattern Recognition, vol.1, pp. 374–380. 1999.
18. Rujul R, Makwana Nita and D Mehta, “Single Image Super-Resolution VIA Iterative Back Projection Based Canny Edge Detection and a Gabor Filter Prior”, International Journal of Soft Computing and Engineering, IJSCE, Vol. 3(1), 2013.
19. H. Engl, M. Hanke, A. Neubauer, “Regularization of Inverse Problems, Dordrecht”, Kluwer Academic Publishers, 1996.
20. N. Nguyen, G. Golub, P. Milanfar, “Blind Restoration/Super Resolution with Generalized Cross-Validation using Gauss-Type Quadrature Rules”, in Conference Record of the -Third Asilomar Conference on Signals, Systems, and Computers, vol. 2, pp. 1257–1261, 1999.
21. Mohamed K, Hardie R, “A Collaborative Adaptive Wiener Filter for Image Restoration using a Spatial Domain Multi-Patch Correlation Model”, Eurasia J Adv Signal Process. 2015.

AUTHOR PROFILE

Dr. M. Nagaraju Naik received his Ph. D from Andhra University College of Engineering (Autonomous), Andhra Pradesh, India, in 2017. Masters Degree (M. Tech) in Digital Systems and Computer Electronics (DSCE) from JNTUA, Anantapur, Andhra Pradesh in 2005, and Bachelor of Technology (B. Tech) from K.S. R. M. College of Engineering, Kadapa, Andhra Pradesh, in 1999. India, India. His interest area Signal, Image and Video Processing, and Antennas.

Mr. P. Raveendrababu received his Masters Degree (M. Tech) in Digital Systems and Computer Electronics (DSCE) from JNTUA, Anantapur, Andhra Pradesh, India, Bachelor of Technology (B. Tech) in ECE from JNTUH, Andhra Pradesh, India. His area of interests Image Processing, Microelectronics & VLSI.